Solvent and Linker Influences on $AQ^{\bullet-}/dA^{\bullet+}$ Charge-Transfer State Energetics and Dynamics in Anthraquinonyl-Linker-Deoxyadenosine Conjugates

Yasser H. A. Hussein,[†,⊥] Neil Anderson,[‡] Tianquan T. Lian,[‡] Ibrahim M. Abdou,[†,⊗] Lucjan Strekowski,[†] Victor A. Timoshchuk,[§] Morteza M. Vaghefi,[∥] and Thomas L. Netzel[†,*]

Department of Chemistry, Georgia State University, P.O. Box 4098, Atlanta, Georgia 30302-4098, Department of Chemistry, Emory University, Atlanta, Georgia 30322, Trilink Biotechnologies, Inc., 9955 Mesa Rim Road, San Diego, California 92121, and ChemCyte Inc., 4206 Sorrento Valley Boulevard, Suite A, San Diego, California 92121

Received: August 6, 2005; In Final Form: February 3, 2006

The goal of this work is to produce high yields of long-lived $AQ^{\bullet-}/dA^{\bullet+}$ charge transfer (CT) excited states (or photoproducts). This goal fits within a larger context of trying generally to produce high yields of long-lived CT excited states within DNA nucleoside conjugates that can be incorporated into DNA duplexes. Depending upon the energetics of the anthraquinonyl (AQ) $^3(\pi,\pi^*)$ state as well as the reduction potentials of the subunits in particular anthraquinonyl-adenine conjugates, CT quenching of the AQ $^3(\pi,\pi^*)$ state may or may not occur in polar organic solvents. In MeOH, bis(3′,5′-*O*-acetyl)-N^6-(anthraquinone-2-carbonyl)-2′-deoxyadenosine (AQCOdA) behaves as intended and forms a $^3(AQ^{\bullet-}/dA^{\bullet+})$ CT state with a lifetime of 3 ns. However, in nonpolar THF the $AQ^{\bullet-}/dA^{\bullet+}$ CT states of AQCOdA are too high in energy to be formed, and in DMSO a $^1(AQ^{\bullet-}/dA^{\bullet+})$ CT state is formed but lives only 6 ps. Although the lowest energy excited state for AQCOdA in MeOH is a $^3(AQ^{\bullet-}/dA^{\bullet+})$ CT state, for N^6-(anthraquinone-2-methylenyl)-2′-deoxyadenosine (AQMedA) in the same solvent it is a $^3(\pi,\pi^*)$ state. Changing the linking carbonyl in AQCOdA to methylene in AQMedA makes the anthraquinonyl subunit harder to reduce by 166 mV. This raises the energy of the $^3(AQ^{\bullet-}/dA^{\bullet+})$ CT state above that of the $^3(\pi,\pi^*)$ in AQMedA. The conclusion is that anthraquinonyl-dA conjugates will not have lowest energy $AQ^{\bullet-}/dA^{\bullet+}$ CT states in polar organic solvents unless the anthraquinonyl subunit is also substituted with an electron-withdrawing group that raises the AQ-subunit's reduction potential above that of AQ. A key finding in this work is that the lifetime of the $^3(AQ^{\bullet-}/dA^{\bullet+})$ CT excited state (ca. 3 ns) is ca. 500-times longer than that of the corresponding $^1(AQ^{\bullet-}/dA^{\bullet+})$ CT excited state (ca. 6 ps).′

Introduction

It is now widely accepted that radical cations (holes) can migrate long distances through the DNA π-stack by a series of short-range hops.[1−7] A major target for oxidative damage to DNA is guanine (G), the base with the lowest ionization energy.[8−10] In their investigations of hole transport, Schuster et al. injected holes ($G^{\bullet+}$) into duplex DNA by photoexciting a covalently attached anthraquinone (AQ) chromophore at the end of a duplex.[11] In particular, AQ was joined to the 5′-end of one DNA strand via a flexible eight-atom long linker.[12] Giese et al. studied both superexchange and multistep hopping mechanisms for hole transport from $G^{\bullet+}$ to the 5′-G in a GGG sequence in DNA where the donor and acceptor sites were separated by A/T base pairs.[13] A recent series of papers has investigated injecting adenine cations ($A^{\bullet+}$ holes) into DNA and subsequently transferring them to other donors such as G or phenothiazine (PTZ).[14−16] In one interesting experiment, naphthaldiimide (NDI) and PTZ were incorporated into the same DNA hairpin and photoexcited to produce $NDI^{\bullet-}/PTZ^{\bullet+}$ photoproducts with lifetimes of hundreds of microseconds.[16] The initial charge transfer (CT) excited state (or photoproduct) in these hairpins was $NDI^{\bullet-}/A^{\bullet+}$ that was separated from a terminal PTZ electron donor by three to seven intervening As. As the number of intervening As increased, the lifetime of the $NDI^{\bullet-}/PTZ^{\bullet+}$ photoproduct increased to 330 μs. Unfortunately, the yield of the latter CT product was at most 1−2% and dropped as its lifetime lengthened. The root cause of the low CT efficiency in this system is that the lifetime of back CT within the primary $NDI^{\bullet-}/dA^{\bullet+}$ excited state is only 4 ps.[17] Clearly this system would be amenable to producing high yields of long-lived CT photoproducts, if NDI could be replaced with a photoacceptor chromophore (PC) for which the initial $PC^{\bullet-}/dA^{\bullet+}$ CT excited-state had a longer lifetime.

With the above objective in mind, this work explores conditions under which a long-lived $AQ^{\bullet-}/dA^{\bullet+}$ CT excited state might be formed in a closely linked anthraquinonyl-2′-deoxyadenosine (AQ-dA) nucleoside conjugate. The effects on the photoinduced CT process due to changing both the type of linker and solvent polarity are explored with a variety of time-resolved and continuous spectroscopic techniques. As will be discussed next, while the $^3(\pi,\pi^*)$ state of AQ (T_1) can readily oxidize guanine, the same is not generally true for adenine and adenosine. What AQ offers that NDI does not is the possibility of forming a triplet $AQ^{\bullet-}/dA^{\bullet+}$ CT excited state that should have a much longer lifetime than a comparable singlet excited state.

$AQ^{\bullet-}/dA^{\bullet+}$ CT State Energetics. Photoexcited AQ-dA nucleoside conjugates could serve as a source of a hole in the

* To whom correspondence should be addressed. E-mail: tnetzel@gsu.edu.
† Georgia State University.
‡ Emory University.
§ Trilink Biotechnologies, Inc.
∥ ChemCyte Inc.
⊥ Current address: P.O. Box 25, Sidi Gaber, 21311, Alexandria, Egypt.
⊗ Current address: UAE University, Department of Chemistry, P.O. Box 17551, Al-Ain, UAE.

10.1021/jp054395q CCC: $33.50
Published on Web 03/16/2006

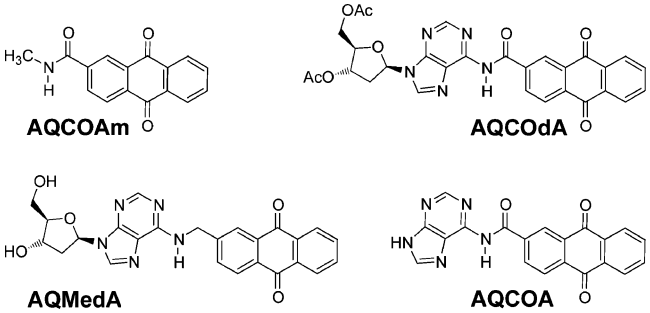

Figure 1. Structural drawings of two AQ-dA nucleoside conjugates, an AQ-A base conjugate, and the spectroscopic AQ model, AQCOAm. Note that 3′,5′-*O*-acetyl groups were added in the case of AQCOdA to improve this nucleoside's solubility in organic solvents.

base stack of a DNA duplex if the free energy of forming the $AQ^{\bullet-}/dA^{\bullet+}$ CT excited state from the T_1 state of AQ (ΔG_{CT}) were less than zero. Equation 1 summarizes this condition as

$$\Delta G_{CT} = -E(T_1) + e[E_{1/2}(dA^{\bullet+}/dA) - E_{1/2}(AQ/AQ^{\bullet-})] + w(r - r_0) \quad (1)$$

where $E(T_1)$ is the energy of the T_1 state of AQ, e is the charge of an electron, $E_{1/2}$ is the electrochemical midpoint (or reduction) potential in volts for the indicated couple, $w(r)$ is the Coulombic work involved in forming the radical pair separated by a distance r, and r is greater than the sum of the donor and acceptor radii (r_0). In polar solvents $w(r)$ is negligible.[18,19]

The energy the T_1 state of AQ is about 2.70 eV (ca. 460 nm).[20] Thus, if the second term in eq 1 is less that 2.70 eV, one would expect CT quenching of the AQ T_1 state. Generally, a ΔG_{CT} value of about −200 meV is sufficiently negative to produce rapid CT quenching. The reduction potential of $AQ/AQ^{\bullet-}$ in dimethylformamide (DMF) is reported to be −0.86 V (versus SCE),[21] while the reduction potential of $dA^{\bullet+}/dA$ in acetonitrile (MeCN) is reported to be 1.72 V (versus SCE).[8] The solvation energy change on going from DMF to MeCN is estimated to be only −0.02 eV[8] and will be neglected here. Substituting the $E(T_1)$ and $E_{1/2}$ values into eq 1 yields ΔG_{CT} equal to −120 meV. Because CT quenching between AQ and dA in polar organic solvents is a close call and because covalently linking AQ and adenine subunits can affect the parameters in eq 1, each AQ-adenine conjugate must be investigated individually to see how it behaves.

Anthraquinonyl-Adenine Conjugate Structures. Figure 1 presents structural drawings of the three anthraquinonyl conjugates and a model anthraquinone that are studied in this work. Both AQCOdA and AQMedA are nucleoside conjugates that are linked via N^6 of adenine and C2 of AQ. In the first, the linker is a carbonyl group, and in the second, it is a methylene group. AQCOA is similar to AQCOdA except that it lacks the sugar of the nucleoside; AQCOAm is spectroscopic model of the AQ group in which dA and A have been replaced with a methyl group except for retention of N^6.

Expectations and Unknowns for Photoinduced CT in AQ-dA Conjugates. Related studies of pyrenyl-2′-deoxyuridine (Py-dU) nucleoside conjugates[22−30] have dealt almost exclusively with singlet excited states, both (π,π^*) and $Py^{\bullet+}/dU^{\bullet-}$ CT types.[22,31] In AQ-dA nucleoside conjugates, there are two important differences compared to Py-dU conjugates. One, the direction of CT is reversed; consequently the desired CT excited state in the former conjugates is $AQ^{\bullet-}/dA^{\bullet+}$ with an oxidized rather than a reduced DNA base as in the latter conjugates. Two, in the former conjugates the excited state to be quenched by CT is the lowest energy $^3(\pi,\pi^*)$ state rather than the lowest energy $^1(\pi,\pi^*)$ state as in the latter ones. By way of background, note that AQ is "special" in that intersystem crossing (ISC) from its lowest energy singlet excited state, a $^1(n,\pi^*)$ state, is so fast (<50 ps) that AQ does not fluoresce.[32] Indeed the extremely fast $^1(n,\pi^*) \rightarrow {}^3(\pi,\pi^*)$ ISC rate is precisely what makes AQ interesting in the context of forming within a nucleoside conjugate a high yield of a ^{3}CT excited state with a lifetime >1 ns. Key questions then become will CT occur from the $^1(n,\pi^*)$ or $^3(\pi,\pi^*)$ state and, if from the latter, how long will the resulting ^{3}CT state live.

On the basis of extensive investigation of the solvent dependence of $^1(Py^{\bullet+}/dU^{\bullet-})$ CT energetics and dynamics in Py-dU conjugates, one reasonably expects that CT quenching of the $^3(\pi,\pi^*)$ states in AQ-dA conjugates to form $^3(AQ^{\bullet-}/dA^{\bullet+})$ CT states will be more favorable in polar solvents such as MeCN and methanol (MeOH) and less favorable in nonpolar solvents such as tetrahydrofuran (THF). In MeOH hydrogen bonding to the carbonyl groups in the $AQ^{\bullet-}$ subunit of the $AQ^{\bullet-}/dA^{\bullet+}$ CT state might add additional CT state stabilization in excess of that seen in the polar but not hydrogen bonding solvent MeCN (see more below). Importantly, only locally excited, pyrenyl (π,π^*) states and pyrene → dU CT states have been observed experimentally in pyrenyl-dU nucleosides and identified in computations[25,27,33] of pyrenyl-dU nucleoside models. In particular, states arising from excitation of electrons in amido-linker orbitals to empty dU orbitals or of electrons in pyrenyl orbitals to empty amido-linker orbitals were not seen. Presumably such "linker" CT transitions were energetically unfavorable. However in AQ-dA nucleoside conjugates, AQ is ca. 1.1 V easier to reduce than dU in Py-dU conjugates. Thus states arising from excitation of electrons in amido-linker orbitals to empty AQ orbitals ($AQ^{\bullet-}/Am^{\bullet+}$ CT) may be low enough in energy to be kinetically important in AQ-dA conjugates.

Potentially important excited states in AQ-dA conjugates include the singlet and triplet (n,π^*) states, singlet and triplet (π,π^*) states, the hoped for lowest energy $^3(AQ^{\bullet-}/dA^{\bullet+})$ CT state, and new singlet and triplet $AQ^{\bullet-}/Am^{\bullet+}$ CT states. Considering polarity, the least polar states are the (n,π^*) and (π,π^*) states; $AQ^{\bullet-}/Am^{\bullet+}$ CT states should be modestly polar, whereas $AQ^{\bullet-}/dA^{\bullet+}$ CT states should be very polar. Thus in nonpolar solvents $AQ^{\bullet-}/dA^{\bullet+}$ CT states should be much higher in energy than in polar solvents. In contrast, the energies of (n,π^*) and (π,π^*) states should vary only modestly as solvent polarity is changed. The energies of $AQ^{\bullet-}/Am^{\bullet+}$ CT states should be stabilized somewhat more than those of (n,π^*) and (π,π^*) states as solvent polarity is increased, but much less than those of $AQ^{\bullet-}/dA^{\bullet+}$ CT states. Finally note that hydrogen bonding was very stabilizing for $Py^{\bullet+}/dU^{\bullet-}$ CT states in Py-dU nucleosides, because it did not also stabilize the pyrenyl (donor) subunit in the ground state. This is not likely to be the case for $AQ^{\bullet-}/Am^{\bullet+}$ CT states, because hydrogen bonding can stablize both the amido (donor) linker in the ground state as well as the carbonyls of $AQ^{\bullet-}$ in the $AQ^{\bullet-}/dA^{\bullet+}$ CT state.

Our goal in this study to develop excited-state energy level diagrams that categorize the important excited state changes that occur to the above types of states in AQ-dA conjugates as solvent polarity and hydrogen bonding capability are changed. These diagrams, however, will not be complete electronic manifolds of these molecules. Rather, generation of complete excited state, energy level representations will necessitate theoretical studies along the lines of INDOs CIS discrete reaction field (DRF) computations[34] that employ explicit solvent models

to analyze the electronic structures of ensembles of thermally accessible solute/solvent configurations generated via molecular dynamics.[33]

Materials and Methods

General Synthetic Methods. MeOH, MeCN, THF, and dimethyl sulfoxide (DMSO) solvents were purchased from Burdick & Jackson (spectroscopic or HPLC grade) and used as received. Other reagents, chemicals, and solvents were obtained from common suppliers and were usually used without further purification. AQCOAm, AQCOdA, and AQCOA were synthesized as described by Abdou et al.[35] AQMedA was synthesized as described below. High-resolution EI (electrospray ionization) MS were recorded in positive ion mode at the Mass Spectrometry Laboratory of the Georgia Institute of Technology. NMR spectra were recorded on a Varian Unity +300 using DMSO-d_6 as solvent at GSU. Chemical shifts for ^{1}H NMR were recorded relative to DMSO (2.49 ppm).

Synthesis of AQMedA. N^9-(β-D-2-Deoxyribofuranosyl)-N^6-(anthraquinone-2-methylenyl)adenine (AQMedA). N^9-(β-D-2-Deoxyribofuranosyl)-6-chloropurine (200 mg, 0.74 mmol) was suspended in *n*-butanol (20 mL) and heated under reflux with 2-aminomethylanthraquinone hydrobromide (600 mg, 2.1 mmol, 2.8 equiv) and triethylamine (0.5 mL, 5 equiv). After 2 h the mixture was evaporated to dryness. Coevaporation of the residue from xylenes and purification by silica gel column chromatography (80 mL, eluted with a mixture of dichloromethane/methanol 95:5 v/v) afforded the desired product as a yellow foam (270 mg, 77% yield, 96% purity by reverse-phase HPLC). ^{1}H NMR (300 MHz, DMSO-d_6): δ(ppm) 8.68 (s, 1H, N^{6}H), 8.40 (s, 1H, H$_8$), 8.12−8.20 (m, 5H, H$_2$/H$_{5''-8''}$), 7.84−7.94 (m, 3H, H$_{1'',3'',4''}$), 6.35 (t, 1H, J = 6.7 Hz, H$_{1'}$), 5.30 (d, 1H, J = 3.9 Hz, OH$_{3'}$), 5.17 (t, 1H, J = 5.6 Hz, OH$_{5'}$), 4.87 (s, 2H, CH$_2$-linker), 4.40 (s, 1H, H$_{3'}$), 3.86−3.87 (m, 1H, H$_{4'}$), 3.47−3.63 (m, 2H, H$_{5'\alpha}$/H$_{5'\beta}$), 2.68−2.78 (m, 1H, H$_{2'\alpha}$), 2.22−2.30 (m, 1H, H$_{2'\beta}$). UV, λ_{max} (MeOH) 256, 265, 272 (sh), 326 nm. ^{13}C NMR (75 MHz, DMSO-d_6): δ(ppm) 182.60, 182.23, 152.33, 147.42, 139.87, 134.53, 134.44, 133.06, 131.76, 127.09, 126.73, 126.70, 124.90, 88.01, 83.93, 70.92, 61.84. HR ESI MS *m*/*z* (M$^+$): $C_{25}H_{21}N_5O_5$ Calc′d 471.15427, found 471.15430.

2-Aminomethylanthraquinone Hydrobromide. 2-Bromomethylanthraquinone (1 g, 3.3 mmol) was dissolved in hot dimethylformamide (50 mL) and, after a careful cooling to prevent crystalization, treated with a saturated solution of methanolic ammonia. The crude product was crystallized, filtered, washed with MeOH, and dried to give 1 g of the desired product, which was used without a further purification to make AQMedA.

UV−Visible Absorbance Spectroscopic Methods. Absorbance spectra were recorded on a Shimadzu UV 2501PC high performance spectrophotometer equipped with a double monochromator for reduced stray light. The spectral bandwidth (SBW) for absorbance spectra was 1 nm, and sample concentrations are given in the figure captions. Molar absorption coefficients (ϵ) of anthraquinonyl compounds were measured by weighing a 2−3 mg sample to ±0.01 mg and dissolving it by stirring for one week in a 100-mL volumetric flask with the desired solvent. Quantitative dilutions were made to produce Beer's law plots for ϵ calculation. The ϵ values for AQCOAm, AQCOdA, AQCOA, and AQMedA in a number of solvents are given in Table 1S.

UV−Visible Emission Spectroscopy and Emission Quantum Yield Methods. Except where noted otherwise, samples for emission measurements were deoxygenated by bubbling solvent-saturated nitrogen gas into a quartz cuvette equipped with an open-screw cap and a Teflon-silicone septum (Wilmad Glass, Part # WG-9F/OC-Q-10) for 20−30 min while stirring. Emission spectra were recorded on PTI (Photon Technology International, Inc.) QuantaMaster-1 spectrofluorometer using 5-nm excitation and emission SBWs. Generally spectra were recorded from 340 to 625 nm at 0.5 nm intervals using 5-s integration times at each wavelength. All samples were excited at 326 nm in 1-cm quartz cuvettes using a right-angle excitation and emission geometry (A_{326} was 0.065−0.10). Polarization artifacts were avoided by positioning an achromatic depolarizer in the excitation beam and recording emission spectra through a polarizer adjusted to 54.7° with respect to vertical. All spectra were corrected for the wavelength dependent emission sensitivity of the fluorometer using appropriate wavelength correction factors (W/cm^2 units) developed at GSU. Additionally, all spectra were corrected for possible variation of excitation intensity by normalization with respect to the intensity of Raman scattering from deioninzed water. A description of the method used to calculate relative emission quantum yields for AQMedA in various solvents is given in the Supporting Information.

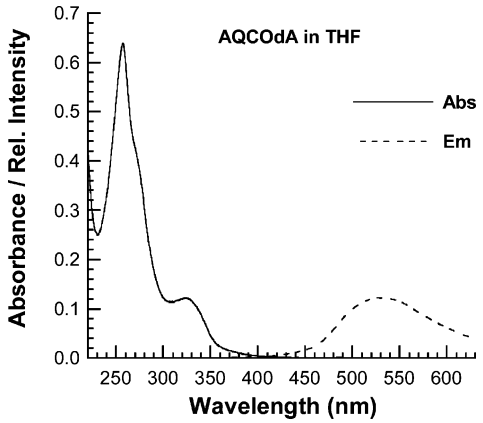

Figure 2. Absorbance and relative emission spectra for AQCOdA in deoxygenated THF; sample concentrations in 1-cm path length cells were, respectively, 1.4 × 10^{-5} M and 7.4 × 10^{-6} M for absorbance and emission experiments.

Results

Absorbance and Emission Spectra for AQCOdA in THF. Figure 2 presents absorbance and emission spectra for AQCOdA in THF. Importantly, the absorbance spectra for AQCOdA, AQCOAm (lacking adenine), and AQ itself are nearly identical to each other. However, while AQCOdA emits in THF, neither AQCOAm nor AQ emit in any solvent.[32] In AQ the lowest electronic singlet excited state is $^1(n,\pi^*)$, and it rapidly (<50 ps) intersystem crosses to the $^3(\pi,\pi^*)$ manifold.[36] This rapid loss of singlet state population renders AQ emissionless at room temperature. Clearly the fact that AQCOdA emits in THF means that a new type of lowest energy singlet excited state is present in the molecule that is not present in AQ. Other substituted AQs do emit, however, such as 1,4-diaminoanthraquinone.[32] In amine-substituted AQs, the lowest energy excited singlet state is an amine-to-AQ CT state. Whereas the $^1(n,\pi^*)$ state in AQ has an ultrafast ISC rate to the $^3(\pi,\pi^*)$ state, the singlet amine-to-AQ CT state does not. Rather, it lives long enough to fluoresce. By anlogy with amine-substituted AQs and for convenience of discussion, we assign the fluorescent, lowest energy singlet state in AQCOdA as arising from excitation of electrons in amido orbitals to empty AQ orbitals ($AQ^{\bullet-}/Am^{\bullet+}$ CT). As noted in the Introduction section, AQ is ca. 1.1 V easier

to reduce than dU. Thus it is reasonable to expect low energy $AQ^{\bullet-}/Am^{\bullet+}$ CT states to be kinetically important in AQ-dA conjugates.

Figure 1S presents expanded views of the absorbance spectra of both AQCOAm and AQCOdA in THF, DMSO, and MeOH. Note that the strong band in the 325-nm region is an allowed $^1(\pi,\pi^*)$ absorption and that absorption to the $^1(n,\pi^*)$ state in the 460-nm region is forbidden. Both AQCOAm and AQCOdA show the expected red-shift of $^1(\pi,\pi^*)$ absorption on going from THF (nonpolar) to DMSO (polar) solvent. What is striking, however, is that this absorption is strongly blue-shifted with respect to its location in DMSO on going to MeOH, even though MeOH is also a polar solvent. Evidence that the 325-nm $^1(\pi,\pi^*)$ state in these two compounds is likely strongly mixed with a new $^1(AQ^{\bullet-}/Am^{\bullet+})$ CT state is provided by the molar absorption (ϵ) data in Table 1S, where the absorption of AQCOAm varies nearly a factor of 2.5 on going from MeOH ($\epsilon_{325} = 3.9$ mM^{-1} cm^{-1}) to THF ($\epsilon_{324} = 9.6$ mM^{-1} cm^{-1}). Most likely the strong blue-shift of the long-wavelength absorption edge of the 325-nm band in AQCOAm and AQCOdA on going from DMSO to MeOH is due to solute/solvent hydrogen bond interactions that are present in MeOH but absent in DMSO.

An important feature in the absorbance spectra of AQCOdA shown in the bottom panel of Figure 1S is increased absorbance in the 370−440 nm region compared to that for AQCOAm. Certainly the extent of amido conjugation is extended in AQCOdA compared to AQCOAm. Aditionally, the possibility of $AQ^{\bullet-}/dA^{\bullet+}$ CT transitions is now real in the former compound. Although $AQ^{\bullet-}/dA^{\bullet+}$ CT transitions are forbidden and thus have very small oscillator strength, they can borrow intensity from nearby allowed transitions. This may well be happening in the 370−440 nm region for AQCOdA. As for AQCOAm in the top panel of Figure 1S, changing solvent for AQCOdA from DMSO to MeOH blue-shifts both the long-wavelength edge of the 325-nm absorbance band and as well lessens the strength of the new 370−440 nm absorbance. Again solute/solvent hydrogen bond interactions in MeOH appear to be the likely cause.

Femtosecond TA Spectra and Kinetics for AQCOdA in THF. Figure 3 presents transient absorbance (TA) spectra at three times after photoexcitation at 400 nm with a ca. 250-fs duration (fwhm) laser pulse (top panel) and TA kinetics at 640 nm (bottom panel) for AQCOdA in THF. Two TA decay processes are seen in Figure 3 and throughout the 460−680 nm region: 16 ps and 1.9 ns. The TA spectra show that excited state absorbance features for both of these relaxations are substantially the same. Figure 2S replots these same TA spectra normalized at 520 nm. The normalized TA plots show that the main difference between the shapes of the TA spectra is that the absorbance at longer times is blue-shifted with respect to the absorbance at earlier times. Thus the 16-ps relaxation corresponds the solvent relaxation about the charge distribution of the excited state. The 1.9-ns TA decay in THF then is reasonably assigned to the emitting $^1(AQ^{\bullet-}/Am^{\bullet+})$ CT state of AQCOdA. Having said this, we must recognize that in THF there is no evidence of $AQ^{\bullet-}/dA^{\bullet+}$ CT state formation. Certainly, the nonpolar nature of THF significantly raises the energy of $AQ^{\bullet-}/dA^{\bullet+}$ CT states relative to their energy in more polar solvents. Importantly, CT states with the largest dipoles will be both destabilized most in nonpolar solvents and stabilized most in polar ones.

Figure 4 presents an energy level diagram for AQCOdA in THF that summarizes the above discussion. In it the fluorescent $^1(AQ^{\bullet-}/Am^{\bullet+})$ CT state is shown as the lowest energy singlet excited state, and the $^1(AQ^{\bullet-}/dA^{\bullet+})$ CT state is shown at higher energy than the $^1(AQ^{\bullet-}/Am^{\bullet+})$ CT state. We do not know the exact location of the $^1(AQ^{\bullet-}/dA^{\bullet+})$ CT state with respect to the $^1(n,\pi^*)$ state, but suspect that the $^1(AQ^{\bullet-}/dA^{\bullet+})$ CT lies above the $^1(n,\pi^*)$ state as shown in the figure. The 1.9-ns lifetime of the $^1(AQ^{\bullet-}/Am^{\bullet+})$ CT state allows ample time for ISC to its $^3(AQ^{\bullet-}/Am^{\bullet+})$ CT state. We also do not know the exact location of the $^3(AQ^{\bullet-}/Am^{\bullet+})$ CT state with respect to the $^3(\pi,\pi^*)$ state, but suspect that it lies below the $^3(\pi,\pi^*)$ as implied in the figure. The question mark by the ISC relaxation between the singlet and triplet $AQ^{\bullet-}/Am^{\bullet+}$ CT states indicates that the time window of the femtosecond TA experiments did not permit observing

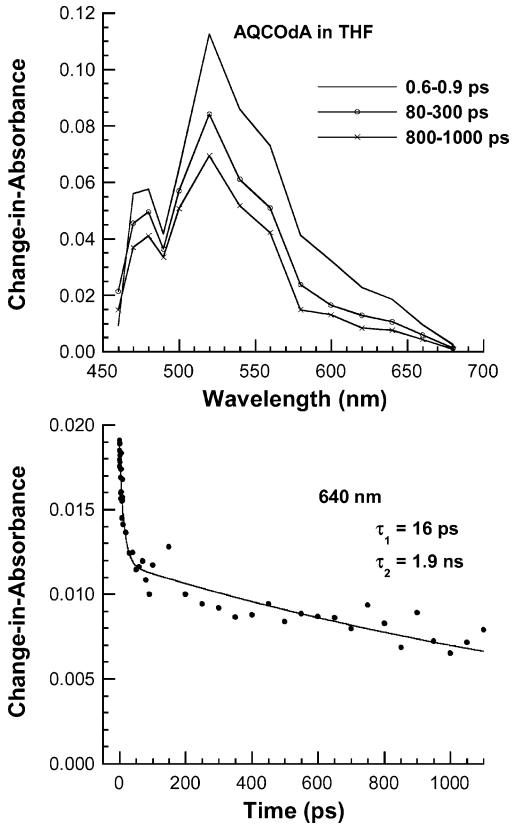

Figure 3. TA kinetics for 5.0 mM AQCOdA in THF following photoexcitation at 400 nm with a ca. 250-fs duration (fwhm) laser pulse: (top) TA spectra averaged over the indicated time intervals after excitation (data points joined with straight lines) and (bottom) TA kinetics at 640 nm (solid circles are data points, and the solid line is a least-squares fit). The fitting equation in the bottom panel was a sum of two exponentials with zero constant term ($R = 0.98$): (0.070) 16 ± 5 ps and (0.012) 1.9 ± 0.5 ns.

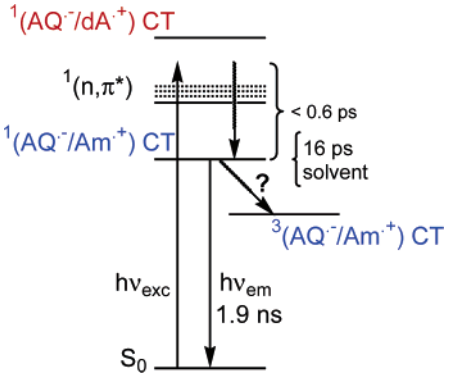

Figure 4. Excited-state energy level diagram for AQCOdA in THF. The question mark indicates that the time window of the femtosecond TA experiment did not allow observation of this state.

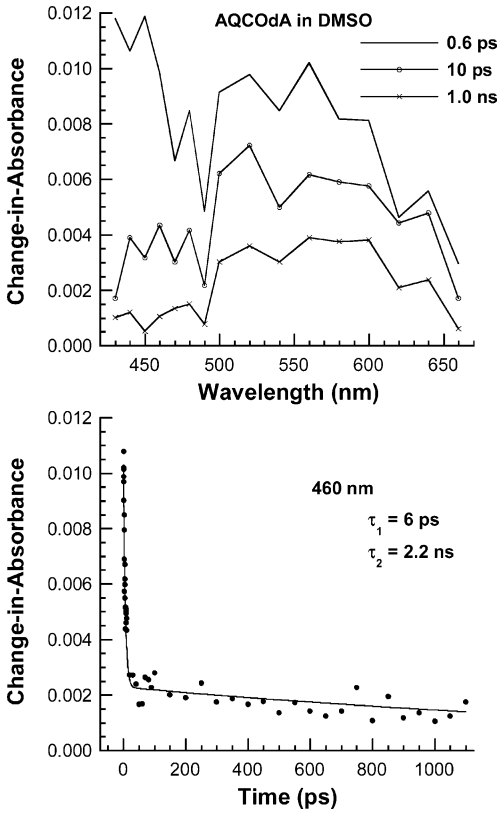

Figure 5. TA kinetics for 4.5 mM AQCOdA in DMSO following photoexcitation at 400 nm with a ca. 250-fs duration (fwhm) laser pulse: (top) TA spectra for the indicated times after excitation (data points joined with straight lines) and (bottom) TA kinetics at 460 nm (solid circles are data points, and the solid line is a least-squares fit). The fitting equation in the bottom panel was a sum of two exponentials with zero constant term ($R = 0.99$): (0.0087) 6 ± 1 ps and (0.0023) 2.2 ± 1.1 ns.

the TA spectrum of the $^3(AQ^{\bullet-}/Am^{\bullet+})$ CT state. One perhaps surprising result is that ultrafast ISC between the $^1(n,\pi^*)$ state and the triplet manifold did not occur in competition with internal conversion within the singlet manifold to populate the fluorescent $^1(AQ^{\bullet-}/Am^{\bullet+})$ CT state. Thus although $^1(n,\pi^*) \rightarrow {}^3(\pi,\pi^*)$ ISC may be ultrafast, internal conversion within the singlet excited-state manifold is even faster for AQCOdA in THF.

Femtosecond TA Spectra and Kinetics for AQCOdA in DMSO. As noted above AQCOdA does not emit in DMSO and MeOH. Clearly the $^1(AQ^{\bullet-}/Am^{\bullet+})$ CT state seen above in THF is no longer the lowest energy singlet state for AQCOdA in these two polar solvents. Two possibilities immediately come to mind. One, the $^1(n,\pi^*)$ state may again be the lowest singlet state, or two, perhaps an $AQ^{\bullet-}/dA^{\bullet+}$ CT state is now the lowest energy excited state. Figure 5 presents TA spectra for AQCOdA in DMSO at three times after photoexcitation at 400 nm with a ca. 250-fs duration (fwhm) laser pulse (top panel) and TA kinetics at 460 nm (bottom panel). Two TA decay processes are seen in Figure 5 and through out the 440−660 nm region: 6 ps and 2.2 ns. In contrast to the TA spectra in Figure 3, the TA spectra in Figure 5 show that excited-state absorbance features are not the same for these two relaxations. Also, the 6-ps TA spectrum in Figure 5 is not similar to that of the $^1(AQ^{\bullet-}/Am^{\bullet+})$ CT state seen in Figure 3. Rather, the highly structured absorbance bands throughout the visible region for the 6-ps transient have features in the 450−650 region that are similar to those of $AQ^{\bullet-}$ in dimethylformamide (DMF).[37] The radical cation of dA has a strong absorption in the 350−400 nm region

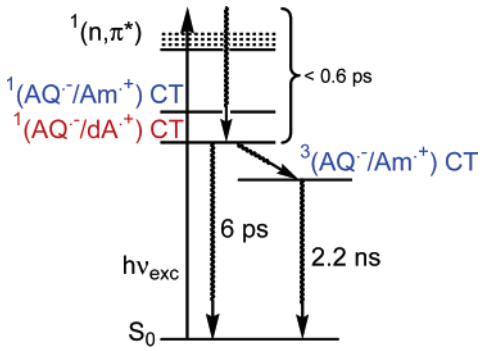

Figure 6. Excited-state energy level diagram for AQCOdA in DMSO.

and a broad moderate absorption from 400 to 600 nm in MeCN.[38] Thus it too can contribute to the TA of an $AQ^{\bullet-}/dA^{\bullet+}$ CT state. On the basis of the similarity with $AQ^{\bullet-}$ absorption features, it appears reasonable to assign the 6-ps TA spectrum for AQCOdA in DMSO to the $AQ^{\bullet-}/dA^{\bullet+}$ CT state. Relatedly, the singlet $pyrene^{\bullet+}/dU^{\bullet-}$ CT state in PAdU has a lifetime of only 5.6 ps in MeCN.[22]

The decay of the short-lived $AQ^{\bullet-}/dA^{\bullet+}$ CT state yields a second excited state with a lifetime of 2.2 ns. The TA of the second state looks neither like that of the initial $AQ^{\bullet-}/dA^{\bullet+}$ CT state nor that of the anthraquinonyl $^3(\pi,\pi^*)$ state.[39] In this circumstance, reasonable assignments are either the $^1(AQ^{\bullet-}/Am^{\bullet+})$ or $^3(AQ^{\bullet-}/Am^{\bullet+})$ states. If AQCOdA fluoresced in DMSO, the former would be the correct assignment. However, since the nucleoside does not emit in DMSO, it appears that the $^3(AQ^{\bullet-}/Am^{\bullet+})$ assignment is more reasonable.

Figure 3S presents femtosecond TA spectra and kinetics plots for AQCOA (lacking the sugar in AQCOdA) in DMSO. As in Figure 3 for AQCOdA in DMSO, AQCOA has two TA decay processes through out the 440−700 nm region: 5.5 ps and 1.9 ns. The final state for AQCOA looks remarkably like the final state for AQCOdA. This is reasonable for two anthraquinonyl $AQ^{\bullet-}/Am^{\bullet+}$ CT states as this type of state would be much the same in these two compounds. The initial TA spectrum for AQCOA is again highly structured as was the case for AQCOdA, but for AQCOA it absorbs more strongly in the 600−660 nm region (maximizing near 700 nm) than in the 500-nm region, whereas for AQCOdA the TA decreases from 560 to 660 nm. Similarly to the TA spectrum of AQCOA, the TA spectrum of the adenine radical cation in aqueous solution shows rising absorbance beginning at 480 nm that maximizes past 590 nm.[40] In contrast, the TA of dA in MeCN is flat from 400 to 600 nm.[38] Thus the initial TA spectra for AQCOA and AQCOdA in DMSO appear to be due, respectively, to $AQ^{\bullet-}/A^{\bullet+}$ and $AQ^{\bullet-}/dA^{\bullet+}$ CT states, whereas the long-lived state in both compounds appears to be the $^3(AQ^{\bullet-}/Am^{\bullet+})$ CT state.

Figure 6 presents an energy level diagram for AQCOdA in DMSO that summarizes the above discussion. In it the non-fluorescent $^3(AQ^{\bullet-}/Am^{\bullet+})$ CT state is shown as the lowest energy and longest lived excited state; also the $^1(AQ^{\bullet-}/dA^{\bullet+})$ CT state is shown at lower energy than the $^1(AQ^{\bullet-}/Am^{\bullet+})$ CT state. Both the $^1(AQ^{\bullet-}/Am^{\bullet+})$ and $^1(AQ^{\bullet-}/dA^{\bullet+})$ CT states must be below the $^1(n,\pi^*)$ state: the former because it should be located much as it was in THF, and the latter because it is observed as the ca. 6-ps transient. The reason that the $^1(AQ^{\bullet-}/dA^{\bullet+})$ CT lies below the $^1(AQ^{\bullet-}/Am^{\bullet+})$ CT state is that it is more stabilized in DMSO due to its larger dipole moment. Finally, singlet and triplet $AQ^{\bullet-}/Am^{\bullet+}$ CT states are expected to have more spin−orbit splitting compared to the singlet and triplet $AQ^{\bullet-}/dA^{\bullet+}$ states. This is consistent with locating the $^3(AQ^{\bullet-}/Am^{\bullet+})$ CT state as the lowest energy triplet state. For

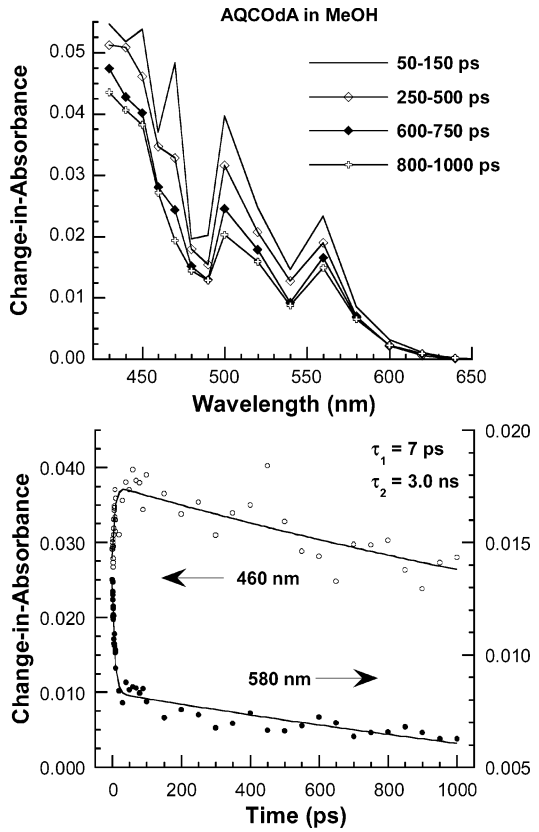

Figure 7. TA kinetics for 5.0 mM AQCOdA in MeOH following photoexcitation at 400 nm with a ca. 250-fs duration (fwhm) laser pulse: (top) TA spectra averaged over the indicated times after excitation (data points joined with straight lines) and (bottom) TA kinetics at 460 nm (open circles) and 580 nm (solid circles). The solid lines are least-squares fits using a sum of two exponentials with zero constant term: 460 nm ($R = 0.80$), (-0.010) 7 ± 2 ps and (0.037) 2.9 ± 0.5 ns; 580 nm ($R = 0.99$), (0.0053) 7 ± 2 ps and (0.0083) 3.2 ± 0.5 ns.

AQCOdA in DMSO as for AQCOdA in THF, internal conversion within the singlet manifold is faster than ISC from the $^1(n,\pi^*)$ state to the triplet manifold. This has the consequence that the $AQ^{\bullet-}/dA^{\bullet+}$ CT state is formed as a singlet via relaxation of the $^1(AQ^{\bullet-}/Am^{\bullet+})$ CT state, and the resulting $^1(AQ^{\bullet-}/dA^{\bullet+})$ CT state has a lifetime of only 6 ps. The key difference between the energy level diagram for AQCOdA in THF (Figure 4) and the diagram for the same nucleoside in DMSO (Figure 6) is that in the latter polar solvent the energy of the $^1(AQ^{\bullet-}/dA^{\bullet+})$ CT state is lowered (or stabilized) to an energy between those of the singlet and triplet $AQ^{\bullet-}/Am^{\bullet+}$ states. The fact that the $^1(AQ^{\bullet-}/dA^{\bullet+})$ CT state lives only 6 ps in DMSO means that the TA of the $^3(AQ^{\bullet-}/Am^{\bullet+})$ CT state is now observable within the time window of the femtosecond TA experiment.

Femtosecond TA Spectra and Kinetics for AQCOdA in MeOH. Both MeOH and DMSO are polar solvents but because MeOH can hydrogen bond with solutes, it can lower the energy of occupied amido linker orbitals as noted earlier in the Introduction section. Additionally, hydrogen bonding will likely have a net stabilizing effect on the energy of the singlet and triplet $AQ^{\bullet-}/dA^{\bullet+}$ CT states of AQCOdA, as was previously observed for $Py^{\bullet+}/dU^{\bullet-}$ CT states in Py-dU nucleosides. Figure 7 presents TA spectra at four times after photoexcitation at 400 nm with a ca. 250-fs duration (fwhm) laser pulse (top panel) and TA kinetics at 460 and 580 nm (bottom panel) for AQCOdA in MeOH. Two relaxation lifetimes are seen in Figure 7 and through out the 430−640 nm region: 7 ps and 3.0 ns. Note that all of the plotted TA spectra are for the decay of the 3-ns lived state. The TA kinetics plots in the bottom panel show

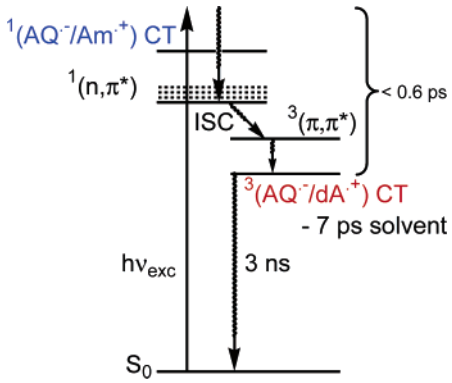

Figure 8. Excited state energy level diagram for AQCOdA in MeOH. The TA kinetics data in Figure 7 show that there is a 7-ps solvent relaxation about the ultra rapidly formed $^3(AQ^{\bullet-}/dA^{\bullet+})$ CT state ($\tau \approx$ 3 ns).

that during the lifetime of the 7-ps species the absorbance increases in the blue region (near 460 nm) and decreases in the red region (near 580 nm). This is the same type of spectral blue-shift that was seen for AQCOdA in THF, and here as there it reflects solvent reorientation about the initially formed excited state. After solvent relaxation the excited state decays with a 3-ns lifetime. The highly structured TA spectrum of the 3-ns lived state with its pronounced absorbance maxima at 500 and 560 nm mark it as due to $AQ^{\bullet-}$. A bit surprisingly at first glance there is almost no absorbance increase beyond 600 nm compared to the TA spectrum observed for the $^1(AQ^{\bullet-}/dA^{\bullet+})$ CT state of AQCOdA in DMSO (Figure 5). The strong blue shift of the $AQ^{\bullet-}/dA^{\bullet+}$ CT state's TA in MeOH compared to DMSO could reflect hydrogen bonding interactions between the nucleoside's $AQ^{\bullet-}/dA^{\bullet+}$ CT state and MeOH. If so, they are consistent with additional stabilization of the $AQ^{\bullet-}/dA^{\bullet+}$ CT state in the latter solvent compared to DMSO. At this time it is important to recall that AQCOdA does not emit in MeOH! If the 3-ns lived state were a singlet state, there would be detectable fluorescence (even from a $^1(AQ^{\bullet-}/dA^{\bullet+})$ CT state as fluorescence from $^1(Py^{\bullet+}/dU^{\bullet-})$ CT states in Py-dU nucleoside conjugates was always readily observable).[22−24,26,41,42] The characteristic $AQ^{\bullet-}$ bands at 500 and 560 nm in the highly structured TA spectrum of the 3-ns lived state in Figure 7 and the lack of emission for AQCOdA in MeOH combine to support assigning the 3-ns lived state as $^3(AQ^{\bullet-}/dA^{\bullet+})$ CT.

Figure 8 presents an energy level diagram for AQCOdA in MeOH that summarizes the above discussion. In it the $^3(AQ^{\bullet-}/dA^{\bullet+})$ CT state is shown as the lowest energy excited state; the $^1(AQ^{\bullet-}/dA^{\bullet+})$ CT state is not shown because it was not observed. The $^1(n,\pi^*)$ state is shown as lowest energy singlet state because presumably it was responsible for ultrafast population of the $^3(\pi,\pi^*)$ state. In turn the $^3(\pi,\pi^*)$ state was most likely rapidly quenched to form the $^3(AQ^{\bullet-}/dA^{\bullet+})$ CT state ($\tau \approx 3$ ns). Key to this sequence of excited-state relaxations was raising of the energy of the $^1(AQ^{\bullet-}/Am^{\bullet+})$ CT state above that of the $^1(n,\pi^*)$ state. Presumably solute/solvent hydrogen bond interactions were responsible for this critical occurrence. In MeOH AQCOdA behaves as the type of AQ-dA conjugate that we had intended to make. It embodies three key conditions: (1) the $^3(AQ^{\bullet-}/dA^{\bullet+})$ CT state is the lowest energy excited state in the compound, (2) the $^1(n,\pi^*)$ state is the lowest energy singlet state, and (3) $^1(n,\pi^*) \rightarrow {}^3(\pi,\pi^*)$ ISC is much faster than charge transfer from the $^1(n,\pi^*)$ state to form the $^1(AQ^{\bullet-}/dA^{\bullet+})$ CT excited state. While we had hoped that the last of these three conditions would be true for AQ-dA conjugates that fulfilled

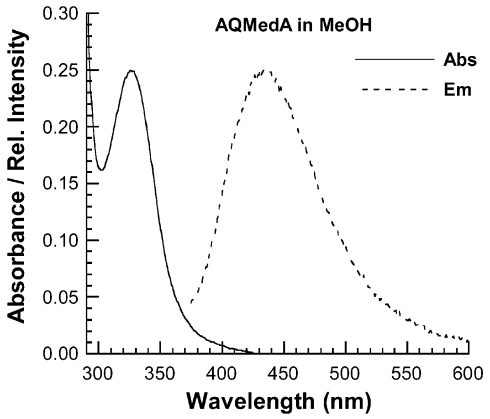

Figure 9. Absorbance and relative emission spectra for AQMedA in MeOH (identical emission for deoxygenated and aerated samples); sample concentrations in 1-cm path length cells were, respectively, 3.0×10^{-5} M and 1.4×10^{-5} M for absorbance and emission experiments.

the first two conditions, it was not obvious a priori that this would be the case.

Two interesting corollaries can be drawn from these findings. The first one is that for AQCOdA in MeOH the time of $^1(n,\pi^*) \rightarrow {}^3(AQ^{\bullet-}/dA^{\bullet+})$ ISC (presumably via the $^3(\pi,\pi^*)$ state) is less than 600 fs. Notably this ISC time that is faster than the time required for MeOH to relax ($\tau \approx 7$ ps) about the solute's $^3(AQ^{\bullet-}/dA^{\bullet+})$ CT excited state. The fact that complete ISC occurs while the solvent is remains thermally equilibrated about the solute's ground-state charge distribution explains why CT did not occur from the $^1(n,\pi^*)$ state: under these circumstances the energy of the $^1(AQ^{\bullet-}/dA^{\bullet+})$ CT state was too high.[33] In support of the above analysis, we note that a similar <500 fs singlet−triplet ISC time was previously reported following photoexcitation of tetrakis(*p*-nitrophenyl)ethylene.[43] The second corollary is that the ca. 3-ns lifetime of the $^3(AQ^{\bullet-}/dA^{\bullet+})$ CT state observed for AQCOdA in MeOH is approximately 500-times longer than the ca. 6-ps lifetime of the corresponding $^1(AQ^{\bullet-}/dA^{\bullet+})$ CT state observed for AQCOdA in DMSO. Thus photoexcitation of an AQ-dA conjugate in a polar solvent can form a $^3(AQ^{\bullet-}/dA^{\bullet+})$ CT excited state in apparently high yield with a lifetime greater than that generally seen for $^1(Py^{\bullet+}/dU^{\bullet-})$ CT excited states in Py-dU nucleosides.

Absorbance and Emission Spectra for AQMedA in MeOH. Figure 9 presents absorbance and emission spectra for AQMedA in MeOH. The shape of the 326-nm absorbance band for AQMedA is identical in THF, MeCN, and MeOH when normalized at 326 nm. Table 1S shows, however, that ϵ_{326} varies a little more than a factor of 2 as the solvent is changed in this series. Similar molar absorption variation with solvent change was also seen for AQCOdA. Such solvent induced ϵ variations in (π,π^*) absorption are consistent with solvent induced changes of the energy of nearby forbidden CT states. The most striking and unexpected aspect of the spectra in Figure 9 is that AQMedA emits in MeOH, and as well in THF and MeCN. The normalized emission spectra in MeOH and MeCN are nearly superimposable with wavelength maxima at 436 nm; these emission spectra are unaffected by switching from deoxygenated to aerated solutions. The relative emission quantum yields in the THF, MeCN, MeOH solvent series are, respectively, 1.0, 0.019, and 0.029. By replacing the linking carbonyl in AQCOdA with methylene in AQMedA, we had hoped to avoid having a singlet linker-to-AQ (^{1}LAQ) CT state below the energy of the $^1(n,\pi^*)$ state. The observed emission for AQMedA suggests that unfortunately a ^{1}LAQ CT state is still present below the $^1(n,\pi^*)$ state even in MeOH! Importantly, substantial (ca. 50-fold) emission quenching for AQMedA on going from THF to MeCN indicates that an $AQ^{\bullet-}/dA^{\bullet+}$ CT state is nearby but higher in energy than the emitting state.

Figure 4S shows that the emission spectrum for AQMedA in THF is substantially different from those in MeOH and MeCN. In fact it appears to be comprised of emission from two states. Upon aeration, most of the long wavelength emission (450−600 nm) is quenched and the short wavelength emission (370−450 nm) is relatively enhanced. Whereas the excited state structure of AQMedA in THF is complicated, it clearly does not have a lowest energy $AQ^{\bullet-}/dA^{\bullet+}$ CT excited state. We will, therefore, make no further attempt to analyze the nature of the emitting states in THF and will instead focus our attention on MeOH.

Nanosecond TA Spectra and Kinetics for AQMedA in MeOH. As noted in the Introduction, whether an $AQ^{\bullet-}/dA^{\bullet+}$ CT state will be below the $^3(\pi,\pi^*)$ state in AQ-dA conjugates in polar solvents is a close call. Additionally, excited state and electrochemical energy considerations took no account of the possible introduction of other new types of excited states below the $^1(n,\pi^*)$ state. For AQCOdA in MeOH, a new $AQ^{\bullet-}/Am^{\bullet+}$ CT state did not intervene between the $^1(n,\pi^*)$ state and the target $AQ^{\bullet-}/dA^{\bullet+}$ CT state, but in DMSO one did. The consequences for the spin (whether a triplet or a singlet) and therefore the lifetime of the ultimately formed $AQ^{\bullet-}/dA^{\bullet+}$ CT state were dramatically different in these two solvents. To better focus on its lowest energy excited state's TA spectrum and lifetime in MeOH, AQMedA was investigated by means of nanosecond TA spectroscopy. In these experiments the excitation pulse was 6-ns long (fwhm), and the excitation wavelength was 341 nm.

Figure 10 presents the TA spectrum seen 15 ns after photoexcitation (top panel) and TA kinetics at 430 and 370 nm (bottom panel) for AQMedA in MeOH. The negative TA signal at 430 nm is due to emission from a ^{1}LAQ CT state and has a lifetime of 4 ns. In contrast the positive TA signal at 370 nm is due to the formation (4 ns) and decay (56 ns) of the longest lived excited state of AQMedA. The TA spectrum of the 56-ns lived final excited state is a good match with that of the $^3(\pi,\pi^*)$ state of AQ itself.[39] Clearly the lowest energy excited state of AQMedA in MeOH is not the desired $AQ^{\bullet-}/dA^{\bullet+}$ CT state. Figure 5S presents a time-expanded look at the 430-nm TA signal along with a plot of the time response of the nanosecond laser system and the convoluted fit to the 430-nm data using a 4-ns lifetime for the emission signal. Significantly, the 430-nm TA data is delayed with respect to the instrument response of the laser system as required for emission from an excited state with a 4-ns lifetime.

Figure 11 presents an energy level diagram for AQMedA in MeOH that summarizes the above discussion. In it the $^3(\pi,\pi^*)$ state is shown as the lowest energy excited state. To account for the 4-ns emission, the ^{1}LAQ CT state is shown as the lowest energy singlet excited state. To account for the 50-fold emission quenching seen on changing solvent from THF to MeCN, the $^1(AQ^{\bullet-}/dA^{\bullet+})$ CT state is placed near but above the ^{1}LAQ CT state. Both the ^{1}LAQ and $^1(AQ^{\bullet-}/dA^{\bullet+})$ CT states are below the $^1(n,\pi^*)$ state as internal conversion within the singlet manifold dominates ISC from the $^1(n,\pi^*)$ state to the $^3(\pi,\pi^*)$ state. In fact the energetics and dynamics of the two lowest energy states in Figure 11 are similar to those seen for common organic fluorophores (see also Figure 4 for AQCOdA in THF); i.e., emission occurs from a lowest energy singlet excited state ($\tau \approx$ a few nanoseconds) that decays both to the ground state and to a longer lived triplet excited state. It differs from many

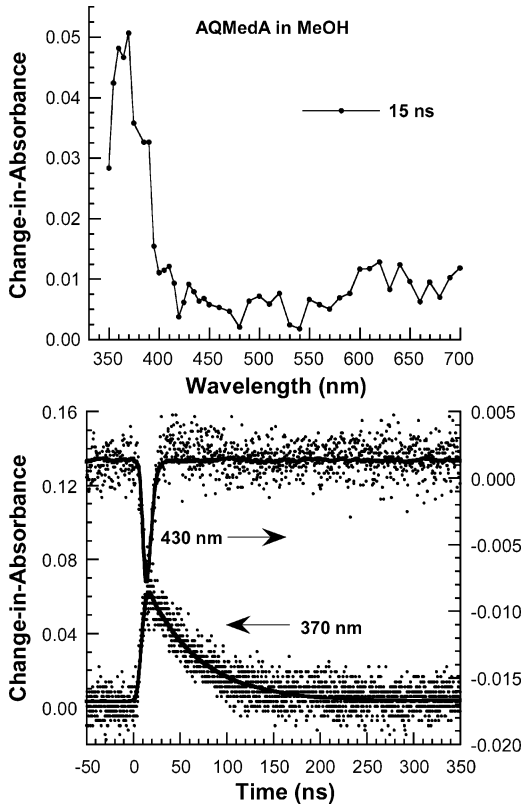

Figure 10. TA spectrum and kinetics for 5.1×10^{-5} M AQMedA in MeOH following photoexcitation at 341 nm with a 6-ns duration (fwhm) laser pulse: (top) TA spectrum averaged over an 8-ns time window centered 15 ns after excitation (data points joined with straight lines) and (bottom) TA kinetics data (closed circles) at 430 and 370 nm as labeled. The solid lines are instrument-response convoluted least-squares fits to the TA data using a either a single exponential or a sum of two exponentials both with a zero constant term: at 430 nm $\tau_1 = 4.1 \pm 0.5$ ns and at 370 nm $\tau_1 = 4 \pm 1$ ns (rise time) and $\tau_2 = 56 \pm 4$ ns (decay). Goodness of fit was judged by uniformity of distributed residuals. See Figure 5S for an expanded plot of the 430 nm TA (emission) kinetics overlayed with the instrument response of the system.

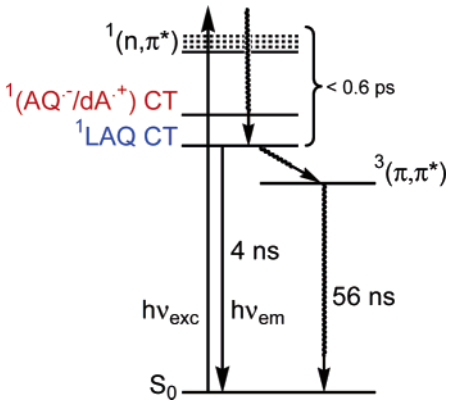

Figure 11. Excited-state energy level diagram for AQMedA in MeOH.

organic fluorophores in that there is a ^{1}(AQ$^{\bullet-}$/dA$^{\bullet+}$) CT state near but above the fluorescing singlet state that significantly quenches emission in polar solvents. Since the lifetime of the ^{1}(AQ$^{\bullet-}$/dA$^{\bullet+}$) CT state is most likely ca. 6 ps, it should not be observable against the TA signal due to the 4-ns lived ^{1}LAQ CT state.

One might reasonably ask, "Why is the lowest energy excited state for AQCOdA in MeOH an AQ$^{\bullet-}$/dA$^{\bullet+}$ CT state, while for AQMedA in the same solvent it is a $^3(\pi,\pi^*)$ state?" The answer is that changing the linking carbonyl in AQCOdA to methylene in AQMedA makes the anthraquinonyl subunit harder to reduce by 166 mV.[25,44] This raises the energy of the AQ$^{\bullet-}$/dA$^{\bullet+}$ CT state above that of the $^3(\pi,\pi^*)$ in AQMedA. Surprisingly, the aminomethylenyl linker still forms a low energy, fluorescent ^{1}LAQ CT state below the $^1(n,\pi^*)$ state. If this were not the case, AQMedA would be as emissionless as AQ itself. We conclude, therefore, that even if an AQ-dA nucleoside conjugate were created without a ^{1}LAQ CT state below the $^1(n,\pi^*)$ state, this conjugate would still not necessarily form a long-lived ^{3}(AQ$^{\bullet-}$/dA$^{\bullet+}$) CT excited state. This is true because unless the AQ subunit were also substituted with an electron-withdrawing group that made it sufficiently easy to reduce, the ^{3}(AQ$^{\bullet-}$/dA$^{\bullet+}$) CT state would be higher in energy than the ultra rapidly formed $^3(\pi,\pi^*)$ state.

Conclusions

The goal of this work is to produce high yields of long-lived AQ$^{\bullet-}$/dA$^{\bullet+}$ CT excited states (or photoproducts). This goal fits within a larger context of trying generally to produce high yields of long-lived CT excited states within DNA nucleoside conjugates that can be incorporated into DNA duplexes. An additional consideration is that such nucleoside conjugates should have at most two linking atoms joining their subunits to enable regiocontrol within an organized series of primary and secondary CT reactions in a multiply covalently labeled DNA duplex assembly.

Analysis of the energetics of ^{3}(AQ$^{\bullet-}$/dA$^{\bullet+}$) CT state formation from the $^3(\pi,\pi^*)$ state of anthraquinonyl-dA nucleososide conjugates indicates that CT quenching between AQ and dA in polar organic solvents is a close call. Depending upon energetics of the AQ $^3(\pi,\pi^*)$ state as well as the reduction potentials of the subunits in particular anthraquinonyl-adenine conjugates, CT quenching of the AQ $^3(\pi,\pi^*)$ state may or may not occur. This paper establishes four main results regarding the ordering of the prominent lowest energy excited states of the AQCOdA nucloside in the solvent series THF, DMSO, and MeOH and of the AQMedA nucleoside in MeOH: (1) for AQCOdA in THF an emissive ^{1}(AQ$^{\bullet-}$/Am$^{\bullet+}$) CT state ($\tau \approx 2$ ns) forms but not an AQ$^{\bullet-}$/dA$^{\bullet+}$ CT state, (2) for AQCOdA in DMSO a ^{1}(AQ$^{\bullet-}$/dA$^{\bullet+}$) CT is formed but is exceedingly short-lived ($\tau \approx 6$ ps), (3) for AQCOdA in MeOH the targeted ^{3}(AQ$^{\bullet-}$/dA$^{\bullet+}$) CT state is formed and lives much longer ($\tau \approx 3$ ns) than the corresponding singlet AQ$^{\bullet-}$/dA$^{\bullet+}$ CT state seen in DMSO, and (4) for AQMedA in MeOH surprisingly the unwanted (but unmistakably identified) $^3(\pi,\pi^*)$ state ($\tau \approx 56$ ns) is formed via an emissive ^{1}LAQ CT state ($\tau \approx 4$ ns).

For AQ-dA compounds in which the anthraquinonyl $^1(n,\pi^*)$ state is the lowest energy singlet excited state, the time of $^1(n,\pi^*) \rightarrow$ ^{3}(AQ$^{\bullet-}$/dA$^{\bullet+}$) ISC is <600 fs; this is faster than MeOH relaxation about an AQ$^{\bullet-}$/dA$^{\bullet+}$ CT excited state. The fact that complete ISC occurs while the solvent is remains thermally equilibrated about the solute's ground-state charge distribution explains why CT does not occur from the $^1(n,\pi^*)$ state for AQCOdA in MeOH: under these circumstances the energy of the ^{1}(AQ$^{\bullet-}$/dA$^{\bullet+}$) CT state is too high.[33] Another key observation in this work is that the ca. 3-ns lifetime of the ^{3}(AQ$^{\bullet-}$/dA$^{\bullet+}$) CT state observed for AQCOdA in MeOH is approximately 500-times longer than the ca. 6-ps lifetime of the corresponding ^{1}(AQ$^{\bullet-}$/dA$^{\bullet+}$) CT state observed for AQCOdA in DMSO. Thus photoexcitation of an AQ-dA conjugate in a polar solvent can form a ^{3}(AQ$^{\bullet-}$/dA$^{\bullet+}$) CT excited state in apparently high yield with a lifetime greater than that generally seen for ^{1}(Py$^{\bullet+}$/dU$^{\bullet-}$) CT excited states in Py-dU nucleosides.

Whereas the lowest energy excited state for AQCOdA in MeOH is a $^3(AQ^{\bullet-}/dA^{\bullet+})$ CT state, for AQMedA in the same solvent it is a $^3(\pi,\pi^*)$ state. Changing the linking carbonyl in AQCOdA to methylene in AQMedA makes the anthraquinonyl subunit harder to reduce by 166 mV.[25,44] This raises the energy of the $AQ^{\bullet-}/dA^{\bullet+}$ CT state above that of the $^3(\pi,\pi^*)$ in AQMedA. Surprisingly, the aminomethylenyl linker still forms a low energy, fluorescent ^{1}LAQ CT state below the $^1(n,\pi^*)$ state. If this were not the case, AQMedA would be as emissionless as AQ itself. In fact the energetics and dynamics of the two lowest energy states of AQMedA in MeOH are similar to those seen for common organic fluorophores; i.e., emission occurs from a lowest energy singlet excited state ($\tau \approx$ a few nanoseconds) that decays both to the ground state and to a longer lived triplet excited state. It differs from many organic fluorphores in that there is a $^1(AQ^{\bullet-}/dA^{\bullet+})$ CT state near but above the fluorescing singlet state that significantly quenches emission in polar solvents. The general conclusion based on comparison of the energetics of the AQCOdA and AQMedA nucleosides is that anthraquinonyl-dA nucleoside conjugates will not have lowest energy $AQ^{\bullet-}/dA^{\bullet+}$ CT states in polar organic solvents unless the anthraquinonyl subunit is also substituted with an electron-withdrawing group that raises the AQ-subunit's reduction potential above that of AQ itself. Unless the AQ subunit is made sufficiently easy to reduce, the $^3(AQ^{\bullet-}/dA^{\bullet+})$ CT state will be located above the $^3(\pi,\pi^*)$ state.

Acknowledgment. We thank the donors of the Petroleum Research Fund, administered by the ACS, for support of this research. T.L.N. thanks Marla Netzel for assistance with literature research.

Supporting Information Available: Femtosecond and nanosecond TA spectroscopic methods; relative emission quantum yield method; absorbance spectra for AQCOAm and AQCOdA in THF, DMSO, and MeOH; molar absorption (ϵ) values for AQCOAm, AQCOdA, and AQCOA in selected solvents; normalized femtosecond TA spectra for AQCOdA in THF; TA kinetics and spectra for AQCOA in DMSO; absorbance and emission spectra for AQMedA in THF; and femtosecond TA kinetics for AQMedA in MeOH. This material is available free of charge via the Internet at http://pubs.acs.org.

References and Notes

(1) Schuster, G. B. *Acc. Chem. Res.* **2000**, *33*, 253−260.
(2) Sanii, L.; Schuster, G. B. *J. Am. Chem. Soc.* **2000**, *122*, 11545−11546.
(3) Giese, B.; Spichty, M. *Chemphyschem* **2000**, *1*, 195−198.
(4) Meggers, E.; Kusch, D.; Spichty, M.; Wille, U.; Giese, B. *Angew. Chem., Int. Ed.* **1998**, *37*, 460−462.
(5) *Long-Range Electron Transfer in DNA I*; Schuster, G. B., Ed.; Topics in Current Chemistry 236; Springer-Verlag: Berlin, 2004.
(6) *Long-Range Electron Transfer in DNA II*; Schuster, G. B., Ed.; Topics in Current Chemistry 237; Springer-Verlag: Berlin, 2004.
(7) Yavin, E.; Boal, A.; Stemp, E. D. A.; Boon, E. M.; Livingston, A. L.; O'Shea, V. L.; David, S. S.; Barton, J. K. *Proc. Natl. Acad. Sci. U.S.A.* **2005**, *102*, 3546−3551.
(8) Seidel, C. A. M.; Schulz, A.; Sauer, M. H. M. *J. Phys. Chem.* **1996**, *100*, 5541−5553.
(9) Steenken, S.; Jovanovic, S. V. *J. Am. Chem. Soc.* **1997**, *119*, 617−618.
(10) Voityuk, A. A. *J. Phys. Chem. B* **2005**, *109*, 10793−10796.
(11) Sartor, V.; Boone, E.; Schuster, G. B. *J. Phys. Chem. B* **2001**, *105*, 11057−11059.
(12) Liu, C.-S.; Hermandez, R.; Schuster, G. B. *J. Am. Chem. Soc.* **2004**, *126*, 2877−2884.
(13) Giese, B. *Acc. Chem. Res.* **2000**, *33*, 631−636.
(14) Kawai, K.; Takada, T.; Tojo, S.; Majima, T. *J. Am. Chem. Soc.* **2003**, *125*, 6842−6843.
(15) Takada, T.; Kawai, K.; Fujitsuka, M.; Majima, T. *Proc. Natl. Acad. Sci. U.S.A.* **2004**, *101*, 14002−14006.
(16) Takada, T.; Kawai, K.; Cai, X.; Sugimoto, A.; Fujitsuka, M.; Majima, T. *J. Am. Chem. Soc.* **2004**, *126*, 1125−1129.
(17) Lewis, F. D.; Kalgutkar, R. S.; Wu, Y.; Liu, X.; Liu, J.; Hayes, R. T.; Miller, S. E.; Wasielewski, M. R. *J. Am. Chem. Soc.* **2000**, *122*, 12346−12351.
(18) Rehm, D.; Weller, A. *Isr. J. Chem.* **1970**, *8*, 259−271.
(19) Rehm, D.; Weller, A. *Ber. Bunsen-Ges. Phys. Chem.* **1969**, *73*, 834−839.
(20) Breslin, D. T.; Schuster, G. B. *J. Am. Chem. Soc.* **1996**, *118*, 2311−2319.
(21) Pletcher, D.; Thompson, T. *J. Chem. Soc., Faraday Trans.* **1998**, *94*, 3445−3450.
(22) Gaballah, S.; Hussein, Y. H. A.; Anderson, N.; Lian, T. T.; Netzel, T. L. *J. Phys. Chem. A* **2005**, *109*, 10832−10845.
(23) Netzel, T. L.; Nafisi, K.; Headrick, J.; Eaton, B. E. *J. Phys. Chem.* **1995**, *99*, 17948−17955.
(24) Netzel, T. L.; Zhao, M.; Nafisi, K.; Headrick, J.; Sigman, M. S.; Eaton, B. E. *J. Am. Chem. Soc.* **1995**, *117*, 9119−9128.
(25) Kerr, C. E.; Mitchell, C. D.; Headrick, J.; Eaton, B. E.; Netzel, T. L. *J. Phys. Chem. B* **2000**, *104*, 1637−1650.
(26) Kerr, C. E.; Mitchell, C. D.; Ying, Y.-M.; Eaton, B. E.; Netzel, T. L. *J. Phys. Chem. B* **2000**, *104*, 2166−2175.
(27) Mitchell, C. D.; Netzel, T. L. *J. Phys. Chem. B* **2000**, *104*, 125−136.
(28) Kaden, P.; Mayer-Enthart, E.; Trifonov, A.; Fiebig, T.; Wagenknecht, H.-A. *Angew. Chem., Int. Ed.* **2005**, *44*, 1636−1639.
(29) Amann, N.; Pandurski, E.; Fiebig, T.; Wagenknecht, H.-A. *Chem. Eur. J.* **2002**, *8*, 4877−4883.
(30) Trifonov, A.; Buchvarov, I.; Wagenknecht, H.-A.; Fiebig, T. *Chem. Phys. Lett.* **2005**, *409*, 277−280.
(31) Triplet (π,π^*) states were formed only in ground-state Py-dU·O_2 complexes. Interestingly, in these dioxygen complexes the rate of ISC from the lowest energy $^1(\pi,\pi^*)$ state to the lowest energy $^3(\pi,\pi^*)$ state greatly exceeded the rate of formation of the $^1(Py^{\bullet+}/dU^{\bullet-})$ CT state.
(32) Petke, J. D.; Butler, P.; Maggiora, G. M. *Int. J. Quantum Chem.* **1985**, *27*, 71−87.
(33) Duijnen, P. T. v.; Netzel, T. L. *J. Phys. Chem. A* **2006**, *110*, 2204−2213.
(34) Grozema, F. C.; Candeias, L. P.; Swart, M.; Duijnen, P. T. v.; Wildeman, J.; Hadziioanou, G.; Siebbles, L. D. A.; Warman, J. M. *J. Chem. Phys.* **2002**, *117*, 11366−11378.
(35) Abdou, I. M.; Netzel, T. L.; Strekowski, L. *Heterocycl. Commun.* **1998**, *4*, 387−391.
(36) Armitage, B.; Yu, C.; Devadoss, C.; Schuster, G. B. *J. Am. Chem. Soc.* **1994**, *116*, 9847−9859.
(37) Fujita, M.; Ishida, A.; Majima, T.; Takamuku, S. *J. Phys. Chem.* **1996**, *100*, 5382−5387.
(38) Ma, J.-H.; Lin, W.-Z.; Wang, W.-F.; Han, Z.-H.; Yao, S.-D.; Lin, N.-Y. *J. Photochem. Photobiol. B* **2000**, *57*, 76−81.
(39) Hulme, B. E.; Land, E. J.; Phillips, G. O. *J. Chem. Soc., Faraday Trans. 1* **1972**, *68*, 2003−2012.
(40) Jovanovic, S. V.; Simic, M. G. *J. Phys. Chem.* **1986**, *90*, 974−978.
(41) Gaballah, S. T.; Collier, G.; Netzel, T. L. *J. Phys. Chem. B* **2005**, *109*, 12175−12181.
(42) Gaballah, S. T.; Vaught, J. D.; Eaton, B. E.; Netzel, T. L. *J. Phys. Chem. B* **2005**, *109*, 5927−5934.
(43) Zijlstra, R. Excited-State Charge Separation in Symmetrical Alkenes. Ph. D., University of Groningen, Groningen, The Netherlands, 2001; p 132.
(44) Hussein, Y. H. A.; Netzel, T. L. Unpublished results. Using cyclicvoltametry (BAS CV-27, 100 mV/s scan speed) with a Pt-electrode in MeCN/0.1 M tetrabutylammonium hexafluorophosphate and ferrocene as an internal standard, we measured the reduction potential of AQCOdA to be 166 mV less negative (easier to reduce) than that of AQMedA. Additionally, under the same CV conditions, AQMedA had the same reduction potential as AQ itself.